Microrheology: Structural evolution under static and dynamic conditions by simultaneous analysis of confocal microscopy and diffusing wave spectroscopy

Yves Nicolas[a)]
Wageningen Centre for Food Sciences, P.O. Box 557, 6700AN Wageningen, The Netherlands and NIZO Food Research, P.O. Box 2, 6710BA Ede, The Netherlands

Marcel Paques[b)]
Wageningen Centre for Food Sciences, P.O. Box 557, 6700AN Wageningen, The Netherlands and Unilever Research and Development Vlaardingen, Postbus 114, 3130AC Vlaardingen, The Netherlands

Alexandra Knaebel, Alain Steyer, and Jean-Pierre Munch
Laboratoire de Dynamique des Fluides Complexes, Institut de Physique, Université de Strasbourg, 3 rue de l'Université 67084 Strasbourg, France

Theo B. J. Blijdenstein
Wageningen Centre for Food Sciences, P.O. Box 557, 6700AN Wageningen, The Netherlands and Levensmiddelenfysica, University of Wageningen, Postbus 8129, 6700 EV Wageningen, The Netherlands

George A. van Aken
Wageningen Centre for Food Sciences, P.O. Box 557, 6700AN Wageningen, The Netherlands and NIZO Food Research, P.O. Box 2, 6710BA Ede, The Netherlands

(Received 18 December 2002; accepted 5 May 2003)

An oscillatory shear configuration was developed to improve understanding of structural evolution during deformation. It combines an inverted confocal scanning laser microscope (CSLM) and a special sample holder that can apply to the sample specific deformation: oscillatory shear or steady strain. In this configuration, a zero-velocity plane is created in the sample by moving two plates in opposite directions, thereby providing stable observation conditions of the structural behavior under deformation. The configuration also includes diffusion wave spectroscopy (DWS) to monitor the network properties via particle mobility under static and dynamic conditions. CSLM and DWS can be performed simultaneously and three-dimensional images can be obtained under static conditions. This configuration is mainly used to study mechanistic phenomena like particle interaction, aggregation, gelation and network disintegration, interactions at interfaces under static and dynamic conditions in semisolid food materials (desserts, dressings, sauces, dairy products) and in nonfood materials (mineral emulsions, etc.). Preliminary data obtained with this new oscillatory shear configuration are described that demonstrate their capabilities and the potential contribution to other areas of application also. © *2003 American Institute of Physics.* [DOI: 10.1063/1.1588747]

I. INTRODUCTION

Studying materials that are deformed is an important new approach to understand product behavior under stress conditions. During deformation, the product structure may change due to internal dynamic processes, e.g., elongation, breakup, and coalescence. Depending on the ingredients and on the processing, the structure will show a physical-chemical arrangement in space of structural elements (fibrils, particles, interfaces). Both the spatial distribution of structural elements and their mutual interaction determine material properties.[1–5] Food systems are highly heterogeneous in their structural arrangement and local domains play a crucial role in product behavior. A range of techniques by which to characterize food microstructure is available, e.g., light and neutron scattering, diffusion and relaxation measurements in nuclear magnetic resonance (NMR), and use of a rheological apparatus. However, these methods reflect the average microstructure in an indirect way. Direct information is still missing on local interactions on a micrometer length scale to link structural elemental behavior to rheological properties. Combining several techniques in an integrated configuration is of value and allows the characterization of structural properties at local length scales. In our definition of ''microrheology'' is the characterization of local structural properties during bulk deformation. It also allows one to trace system behavior back to its origin at the micrometer length scale and identify the ingredients involved and relevant processing parameters. In our approach noninvasive imaging and deformation are combined but the configuration also includes multiple light scatting. Special deformation cells were combined with a confocal scanning laser microscope (CSLM) to study structural behavior over time without being hindered by the

[a)]Corresponding author; current address: DuPont Protein Technologies, Rue Général Patton, Contern L-2984 Luxembourg; electronic mail: ynicolas@protein.com
[b)]Current address: Friesland Coberco Dairy Foods/Corporate Research, P.O. Box 87, 7400 AB Deventer, The Netherlands.

TABLE I. Confocal scanning laser microscope: Main advantages and technical limitations.

Advantages	Technical Limitations
Simultaneous imaging of different items using multiple labeling strategies	Limited in identification of ingredients and structural elements, due to the limited availability of differentiating specific fluorescent probes
Unrivaled image quality due to the confocal principle (no blurring)	Limited optical spatial resolution (submicron)
Observation of dynamic processes and structural evolution	Acquisition frame rate vs image quality
3D volume imaging	
Noninvasive/nondestructive	Limited penetration depth in optical opaque materials

flow of material in the area of observation. We used a concept developed by Taylor in 1934 to obtain a zero-velocity plane in the sample by the countermovement of two elements of the deformation cell.[6] The image plane of the CSLM matches this zero-velocity plane. In the present work, shear is obtained by linear movement of rectangle glasses. Linear movement can also by applied in oscillation. This oscillatory shear configuration allows one to obtain microscopic information and spectroscopic information simultaneously from diffusing wave spectroscopy (DWS), a multiple light scattering technique that determines viscoelastic properties of systems by analysis of the particle mobility.[7–9] This versatile configuration allows the monitoring of the gelation process of milk and model suspensions.[10,11] The configuration is partly based on work previously done by Hébraud *et al.* that introduced combined application of oscillatory deformation with DWS to study the mobility of particles and elastic network properties in concentrated emulsions.[12]

In addition to the above described configuration two other configurations were developed by combining a CSLM with continuous counterrotation and a CSLM with compression/extension.[3,13,14]

The microrheology configurations are of great interest and provide new capabilities for product design, product development, and improvement of product performance based on insight into the underlying structural properties. Examples of industrial issues that can benefit from this approach optimization of the effective ingredient, ingredient replacement while maintaining product performance, and an increase of the number of manufacturing windows, and how to combine stable shelf life with the desired product instability during kitchen handling and oral processing. Examples of scientific issues are elucidation of network formation and network properties (stability, breakdown) or the study of particle interactions (collision, adhesion, coalescence, breakup).

In this article a thorough description of the configuration is given, followed by preliminary data obtained to demonstrate the new capabilities and potential contributions of the configuration to material sciences, industrial research, and product development.

II. DESIGN CONCEPT

A. Confocal scanning laser microscopy

Imaging was performed using an (inverted) Leica confocal scanning laser microscope, model TCS-SP1, configured with an ArKr laser for single photon excitation. The main advantages and drawbacks of the CSLM are summarized in Table I. Rhodamine B solution (CAS 81-88-9, Aldrich Chemical Co., Milwaukee, WI) was used as the fluorescence staining agent for protein and was dissolved in distilled water to a concentration of 0.01%. A 568 nm laser line was used for excitation to induce fluorescence emission detected between 600 and 700 nm. A water immersion objective lens (63×, numerical aperture of 1.2) was used. Its working distance is 220 μm. *Z* scans are performed using a fast piezo objective driving system (Jena MIPOS3-SG, NEMA Electronic BV, The Netherlands).

B. Oscillatory shear cell

The concept of the zero-velocity plane was applied in order to allow analysis without hindering effects of material flow in the area of observation (Fig. 1). Development of the countermovement principle started with Taylor in 1934 using parallel bands and was followed by many other authors.[15–17] New systems were developed using counterrotational cylinders and a cone and plate configuration in counterrotation.[13,18–20]

Here we describe counterlinear shear in oscillation combined with DWS measurements and CSLM observation.

A schematic of the cell is presented in Fig. 2. Detailed schematics of the cell are shown in Figs. 3 and 4 from top and profile views, respectively. The cell consists of two rectangle glass plates aligned parallel driven by piezo elements. The piezo elements drive the upper glass plate and the lower glass plate with a maximum of 90 μm displacement (P-843.60 preloaded closed loop LVPZT translator, Physik Instrumente) and 15 μm displacement (P-843.10 preloaded closed loop LVPZT translator, Physik Instrumente), respectively. Those two piezo elements were selected to obtain a zero-velocity plane close to the lower glass plate when the two piezo elements were used simultaneously to also allow imaging of opaque samples. Each piezo element includes a strain gauge sensor for more accurate displacement. The dimensions of the upper and lower glass plates are $25\times60\times10$ mm and $25\times60\times0.18$ mm, respectively. To reduce friction during movement of the plate, linear bearings are used in the cell (LWRPM/LWRPV, SKF).

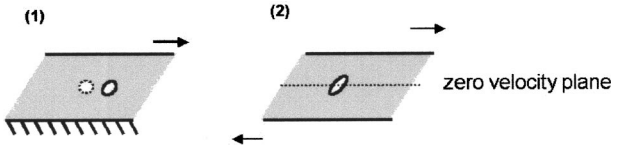

FIG. 1. Concept of zero-velocity plane: (1) only the upper plate moves, (2) both plates move in opposite directions. Undesired movement, with respect to imaging, of the item of interest in (1) is absent in (2).

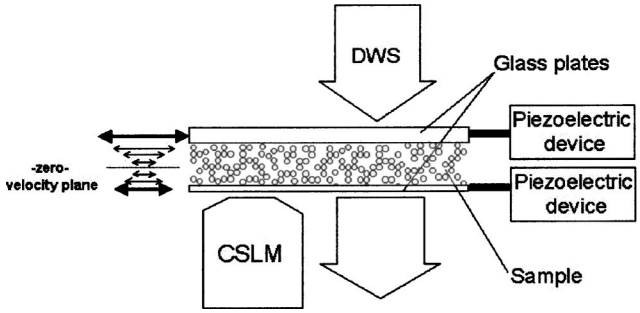

FIG. 2. Schematic of the oscillatory shear configuration including the sample holder which is composed of two glass plates driven by piezos, diffusing wave spectroscopy, and the confocal scanning laser microscope. The arrows on the left show plate movement when both piezos are used to create a zero-velocity plane in the sample.

The minimum adjustable gap size is 120 μm measured by CSLM but smaller sizes can be obtained by increasing the thickness of the lower glass plate. However such a small gap may not allow DWS measurements due to reduction of the photon pathway, which affects the number of scatter events in the sample. The gap size can be increased by adding spacers (Fig. 4 item 24). The flatness of the upper and lower glasses was measured in the middle of the glass at five and six different locations over a total distance of 20 and 25 mm, respectively. The flatness of the upper and lower glass fluctuated 4 and 11 μm in height, respectively.

Measurements of the gap between both glass plates showed less than 4% deviation of the gap value for six different locations (within 0.5 cm^2) indicating a good parallelism between the plates.

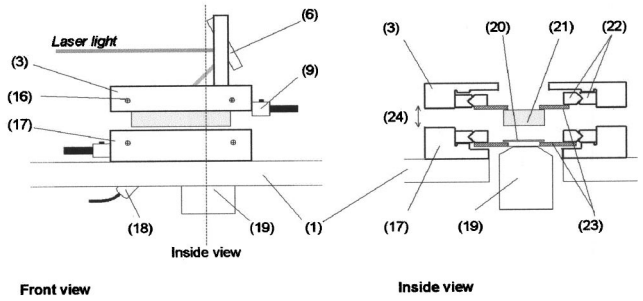

FIG. 4. Detailed front and inside views of the oscillatory shear cell. (1) Basic metal frame; (3) upper metal frame; (6) mirror for diffusing wave spectrometry; (9) connector between the glass support and the spring; (16) screws; (17) lower metal frame; (18) lens collector for DWS in transmission; (19) microscope objective; (20) lower glass plate, 0.2 mm; (21) upper glass plate, 10 mm; (22) linear bearings; (23) metal frame where glass plates are glued; (24) the gap between the two glass plates that can be changed by adding a spacer.

C. Diffusing wave spectroscopy

DWS is a dynamic multiple light scattering technique that is easy to use in opaque particle solutions to monitor particle mobility.[8] It measures the intensity autocorrelation function of multiple scattered light $g_2(\tau)$ as a function of time t for an ergodic system, so the ensemble average is equivalent to an average of the time and is given by

$$g_2(\tau)=\frac{\langle I(t)I(t+\tau)\rangle}{\langle I(t)\rangle^2}, \tag{1}$$

where $I(t)$ denotes the intensity I at time t and τ is the time correlation.[21]

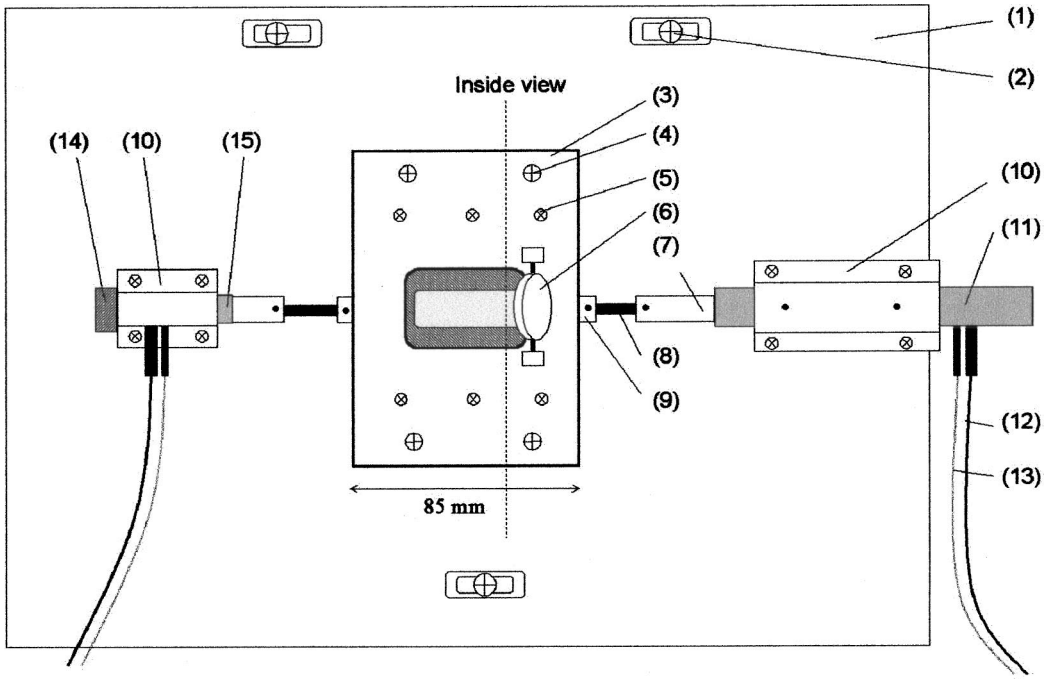

FIG. 3. Schematic top view of the oscillatory shear cell. (1) Basic metal frame; (2) three openings with screws to mount the cell onto the microscope; (3) upper metal frame; (4) four screws to maintain the upper and the lower plate frames after the sample is loaded; (5) six screws to fix linear bearings; (6) mirror for diffusing wave spectrometry; (7) connection between the piezo and the plate; (8) flexible metal cable; (9) connector between the glass support and the flexible metal cable; (10) large and small piezo holders; (11) piezo, 90 μm; (12) amplifier cable; (13) control strain gauge cable; (14) large screw to attach the piezo to its holder; (15) piezo, 15 μm.

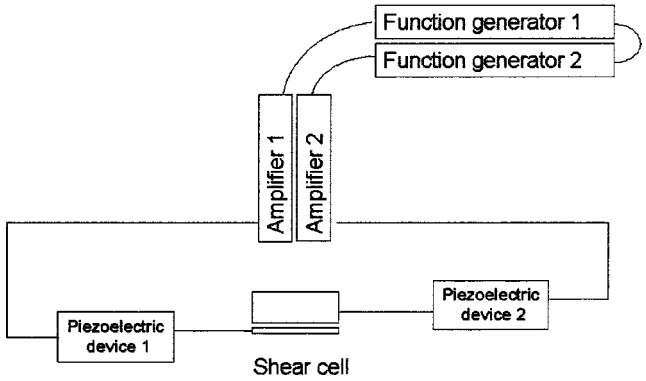

FIG. 5. Configuration of the driving control units to synchronize piezo movement via interlocking of the function generators.

Scattered light detection is easy to implement. A lens collector is placed without laborious precise positioning (precise positioning is not needed for DWS) to collect scattered photons. DWS is used in transmission and in a backscatter setup. A beam expander of 10× (BE10-A, Thorlabs) was used to enlarge the spot from a HeNe laser (Melles Griot, 632.8 nm, 35 mW) to 10 mm in diameter. The laser spot shines the sample into the oscillatory shear configuration using a mirror.

For DWS in transmission, the setup for ''time averaged'' measurements was as follows: the signal of scattered light transmitted was focused by a lens collector (F220FC-B, Thorlabs) and guided into a single mode fiber connected to a photomultiplier tube (ALV SO-SPID, Langen/Hessen, Germany). Fluctuations in intensity were recorded and transferred into intensity correlation functions by a 410R correlator board (Correlator.com, US). The interface between the oscillatory shear cell and the DWS configured for time-averaged analysis is presented in Fig. 4.

For DWS echo measurements the sample was loaded into the oscillatory shear cell and sheared by linear oscillating movement at constant frequency of 100 Hz and different amounts of strain.[12]

For a DWS charge coupled device (CCD) in backscattering a setup for ensemble average measurements is used to study slow relaxation systems and using a CCD camera as the detector can be used to detect speckle patterns during DWS experiments.[22,23] A CCD camera (CF 8/4 1/2 in. Kappa, Gleichen DE) was used with a KTN-CSI camera power supply. A video card (PCI 1408, National Instruments) and LAB-WINDOWS/CVI software (National Instruments) were used to acquire frames at 25 images/s directly on the CCD chip. To obtain the DWS intensity correlation function, pixel-to-pixel intensities were cross correlated from image to image according to the method developed by Knaebel *et al.*[22] The DWS setup for ensemble average measurements is shown in Fig. 5.

III. APPARATUS

A. Oscillatory shear configuration

The oscillatory shear configuration contains the oscillatory shear cell (OSC), a rack for amplifiers, and function generators (Fig. 6). The piezo elements are controlled via the

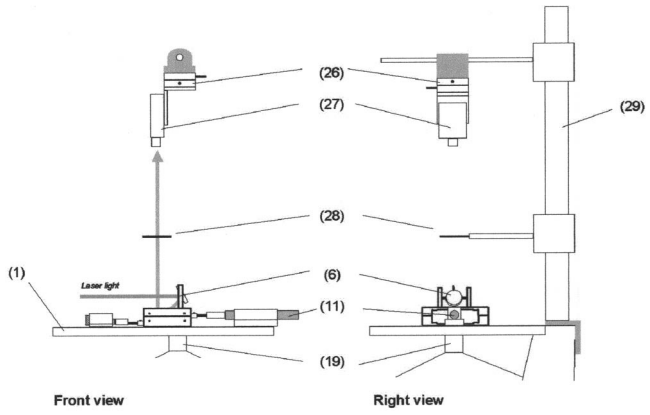

FIG. 6. Detailed front and right side views of the oscillatory shear cell and the CCD camera setup. (1) Basic metal frame; lower metal frame; (11) piezo, 90 μm, (19) microscope objective; (25) $X-Y$ camera stage; (26) CCD camera; (27) pinhole; (28) post for the CCD camera setup.

amplifier rack which contains a strain gauge sensor and a position servo control module (E-509.S3, Physik Instrumente), two amplifier modules (LVPZT, E-505.00, Physik Instrumente), and a display module (E-515.03, Physik Instruments). Piezo movement is set on the function generator (33120A, 15 MHz, Agilent Technologies). The two piezo movements are synchronized by the function generator. Strain of between 0.01% and 88% can be applied depending of the size of the gap and the piezo frequency range (0.05–100 Hz in sinusoidal mode).

B. Temperature control

A temperature control unit (TCAT-1A, Physitemp, US) that includes two infrared lamps (250 W) and a temperature microprobe can be used to set the oscillatory shear cell to a maximum stable temperature of 45 °C.

IV. PERFORMANCE

The OSC combines oscillatory linear deformation, DWS, and the CLSM, and allows simultaneous use of all three functionalities, each combination possible and single use.

A. Sample preparation

Gelatine 10% (w/w) (Pse I, Degussa, Baupte, France) and 10% (w/w) Dextran solution (MW 282 000, Sigma D-7265) in NaCl 0.1 M were dissolved and mixed (ratio of 2/1) at 60 °C. Rhodamine B (0.01%) was added to the mixture. Prior to introducing the sample into the oscillatory shear cell, the cell was heated with the temperature control unit to 45 °C. After loading the preheated sample, the temperature control unit was turned off. The metal cell structure allowed a slow cooling gradient process to obtain the structure desired due to phase behavior: liquid dextran droplets in a continuous gelled gelatine phase.[24]

Low fat milk and 2.4% (w/w) glucono-δ-lactone (G-4750, Sigma) were mixed and 0.5 ml of the mixture was poured into the oscillatory shear cell for DWS measurements

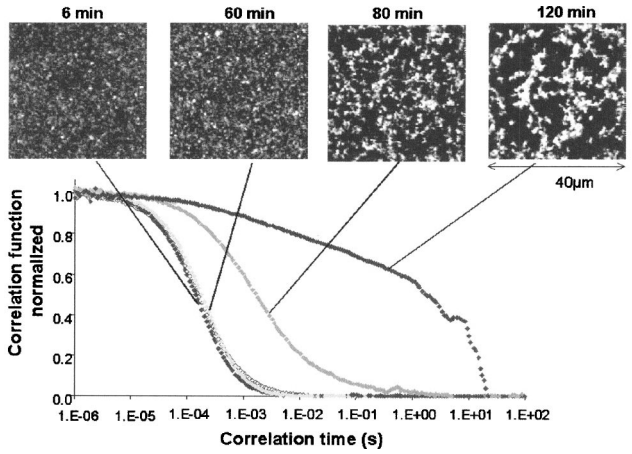

FIG. 7. Oscillatory shear configuration. Simultaneous CSLM observations and DWS time-averaged experiments during acid milk gelation with glucono-δ-lactone (2.4%). The pictures were taken during the gelation process after 6, 60, 80, and 120 min. For each gelation time, DWS experiments were done with a integration time of 2 min and the respective correlation functions are shown.

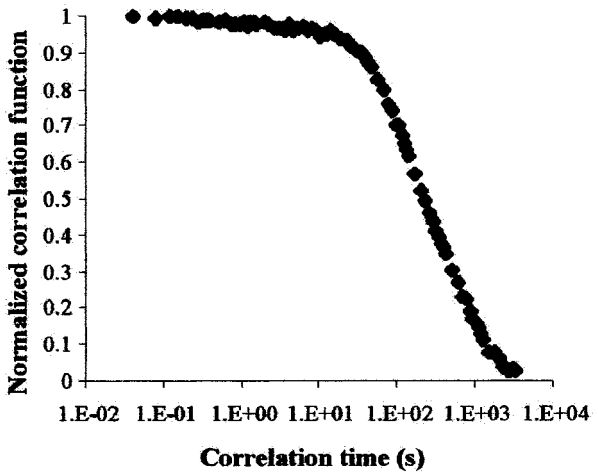

FIG. 8. Diffusing wave spectroscopy measurements using the ensemble average approach with the CCD camera configured of a 30% oil in water emulsion after the addition of 2% Dextran 280 000. With this CCD setup, a well-defined function is described for long correlation times compared to those in Fig. 7.

and simultaneous CLSM observations. Grease was used around the oscillatory shear cell edges to prevent the evaporation of water.

Emulsions 40% (v/v, sunflower oil in water) stabilized with 1% (w/v) whey protein isolate (Bipro, Le Soueur, MN) were made and are described elsewhere.[25] Dextran 2 M (D-5376, Sigma) was added in order to obtain a final concentration of 2% (w/w) in the 30% emulsion. To prevent slippage, the glass plate surfaces were coated for 30 min with poly-L-lysine (P1524, Sigma) 0.1% (w/w water) and washed five times with the same amount of water. Then they were dried and used freshly prepared for experiments.[26]

B. Simultaneous DWS measurements and CSLM observations

Both DWS and CSLM analyses can be done simultaneously to study network formation or breakdown over time. In the experiment the formation of gel of milk protein induced by acidification (proton released over time by the glucono-δ-lactone) was followed over a 120 min period (Fig. 7). After 6, 60, 80, and 120 min, DWS experiments were done for 2 min and CSLM pictures were taken. No correlation functions were present before 6 min because that was the time needed to mix the milk and the glucono-δ-lactone, to load the mixture, and to let it rest. In the DWS correlation function values increased in time for longer correlation times, indicating that the mobility of the main milk protein decreases over time due to network formation and network strengthening. This gelation process was also monitored simultaneously by CSLM observation and showed network formation due to protein aggregation during milk acidification (Fig. 7).

C. Different approaches for slow relaxation processes and fast relaxation processes

In Fig. 7, one can see the system properties changed relatively fast after a defined time (60 min). Thus time integration was set at 2 min to obtain a correlation function of the stable system and correlation function signal above 1.4 at short correlation times (this is not seen in Fig. 7 because the curves were normalized). However, at longer correlation times during gelation, the correlation function was less defined due to the slow relaxation of the system, a reflection of fewer scattering events due to network formation. Application of the DWS-CCD setup in transmission geometry or backscattering geometry dramatically improves definition at longer correlation time intervals (Fig. 8). The oscillatory shear configuration also allows the ''two cell'' DWS technique for nonergodic media (data not shown) and when fast processes occur in a short time as described earlier.[27]

D. DWS for dynamic conditions

Sinusoidal deformation can be applied during DWS experiments to estimate the particle mobility in concentrated emulsions or the network elasticity in flocculated emulsion.[12,28] An oscillation frequency is selected to obtain an echo response during the decrease of the correlation function values [Fig. 9(a)]. This frequency is selected according to network characteristics such as the relaxation time defined

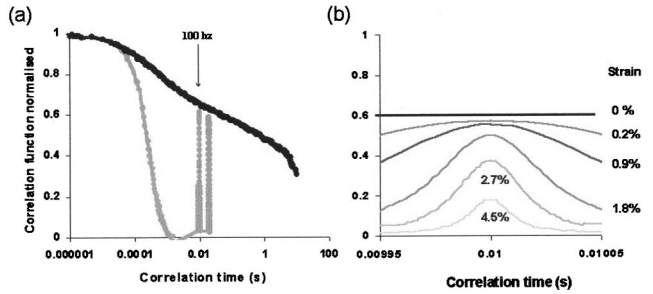

FIG. 9. Oscillatory shear configuration. DWS experiments for a 30% oil in water emulsion after the addition of 2% Dextran. (a) Intensity-cross correlation functions without shear (black symbols) and with shear (gray symbols) (100 Hz, strain 0.23%) and (b) echo measurement at 100 Hz for different amounts of strain.

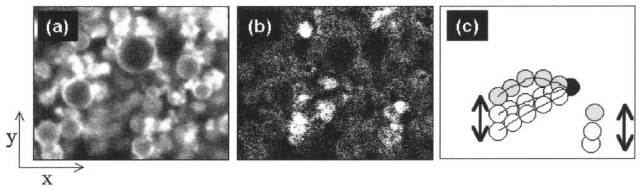

FIG. 10. Interconnectivity of 30% oil in water emulsion after the addition of 2% Dextran in the *Z* projection of a movie acquired 2 μm above the lower glass plate surface while the upper plate oscillates. (a) Sum of seven frames; (b) standard deviation of seven frames (in white are differences during deformation); (c) schematic of particle connectivity (strings) and movement from the light to the dark gray level (arrow); droplets of similar gray levels belong to the same strand. The height is 14 μm. See the text for further explanation.

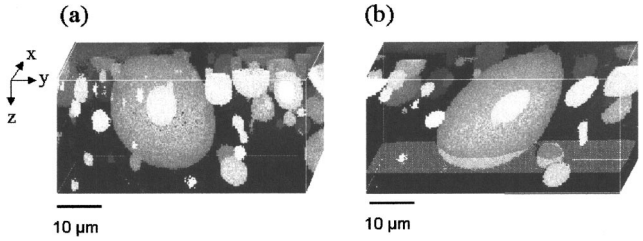

FIG. 11. 3D observation of the zero-velocity plane of Dextran droplets (light) in the gelatin matrix (dark) (a) before shear and (b) during constant shear strain (0.88). The light gray horizontal plane represents the zero-velocity plane.

by the correlation time at a half correlation function value. During oscillation, when the echo peak height decreases, the system properties have changed. Thus in flocculated emulsion, the network elasticity and the mobility of the droplets can be estimated as a function of strain: the correlation value at the maximum peak decreased according to the amount of strain applied [Fig. 9(b)].[28]

E. Observation of the surface properties during deformation

By coating particles or polymer on the OSC glass plates, it is possible to study the connection between the plate surface and the structural elements of the sample. Tribological information can be obtained during deformation and simultaneous CSLM observation at different penetration depths. In Figs. 10(a) and 10(b), the pictures present the addition of seven frames of flocculated emulsion during movement of one plate. To show movement of the particle, standard deviation of the frames was done with IMAGE J software (http://rsb.info.nih.gov/ij/) and the movable particle is shown in white [Fig. 10(b)]. A schematic drawing of particle connectivity and movement during deformation is presented in Fig. 10(c): when the upper glass plate moves, the particle chain made of light particles linked together by a line moved in the *y* direction on the picture and they are represented by different gray levels; the dark particle belonging to the particle chain does not move because it is connected to the surface of the lower glass plate. So the number of particle connections between the glass plate and the bulk of the sample can be estimated over a surface.

F. Observation in the zero-velocity plane during shear

The CSLM allows imaging of a zone in the sample in any optical plane (*xy*, *xz*, or *yz*). When the oscillatory shear cell is used for unidirectional deformation, droplet deformation/relaxation can be observed and interfacial tension can be calculated from data obtained from selected droplets in the image (data not shown). Observations at constant strain can be observed and three-dimensional (3D) image volumes can be reconstructed and they show the zero-velocity plane when deformation in the opposite direction is applied to the sample (Fig. 11). The CSLM allows accurate measurement of the three axes, which is an advantage over the multiple views needed using an optical light microscope.[29]

However, the maximum image frame rate with the CSLM can be a limiting factor in capturing structural features from dynamic processes (e.g., image acquisition during fast deformation) with sufficient image quality (signal to noise ratio and spatial resolution). It depends on the sample properties (transparency, specifics), dynamic or static conditions, signal intensity, and the instrument specifications. Under optimal conditions for the sample and the dye, a maximal frame speed of eight per second was obtained with pixel resolution of 64×64 pixels and a zoom factor of 4. For observation of fast dynamic processes, for which the zero-velocity plane approach is not applicable, the use of a fast acquisition principle is necessary, e.g., a fast scanning laser or Nipkow disk approach.[30]

V. DISCUSSION

The data presented illustrate the versatile capabilities of the microrheology approach, which is a new concept for studying local structural properties of materials to originate bulk behavior to the micrometer length scale, and to overcome the restrictions of present techniques. The detailed description of the oscillatory shear configuration and its capabilities and potential for application, showed the values and benefits of such a configuration for many research and development areas of food and nonfood. It is suitable for the study of a range of systems (emulsions, phase separated biopolymer mixtures, networks), static and dynamic processes, and structural evolution as a function of deformation.

[1] E. A. Gwartney, E. A. Foegefing, and D. K. Larick, J. Food. Sci. **67**, 812 (2002).
[2] I. T. Norton and W. J. Frith, Food Hydrocolloids **15**, 543 (2001).
[3] Y. Nicolas *et al.*, Food Hydrocolloids (to be published).
[4] C. Servais, R. Jones, and I. Roberts, J. Food. Eng. **51**, 201 (2002).
[5] A. Alting, R. J. Hamer, C. G. de Kruif, and R. W. Visschers, J. Agric. Food Chem. **48**, 5001 (2000).
[6] G. I. Taylor, Proc. R. Soc. London **29**, 501 (1934).
[7] D. J. Pine, D. A. Weitz, P. M. Chaikin, and E. Herbolzheimer, Phys. Rev. Lett. **60**, 1134 (1988).
[8] G. Maret, Curr. Opin. Colloid Interface Sci. **2**, 251 (1997).
[9] J. L. Harden and V. Viasnoff, Curr. Opin. Colloid Interface Sci. **6**, 438 (2001).

[10] D. G. Dalgleish and D. S. Horne, Milchwissenschaft **46**, 417 (1991).
[11] P. Schurtenberger, A. Stradner, S. Romer, C. Urban, and F. Scheffold, Chimia **55**, 155 (2001).
[12] P. Hébraud, F. Lequeux, J. P. Munch, and D. J. Pine, Phys. Rev. Lett. **78**, 4657 (1997).
[13] M. Paques, Y. Nicolas, D. van den Ende, J. K. G. Dhont, H. Tromp, R. C. van Polanen, A. van Blaaderen, A. Imhof, and H. Wisman (unpublished).
[14] Y. Nicolas and M. Paques, J. Food Sci. (accepted).
[15] M. L. Krunatz and D. K. Schwartz, J. Rheol. **41**, 1173 (1997).
[16] M. Fermeglier, C. L'Héveder, P. Jenffer, and J. H. E. Promislow, J. Rheol. **42**, 225 (1998).
[17] A. C. Rust and M. Manga, J. Colloid Interface Sci. **249**, 476 (2002).
[18] N. Grizzuti and O. Bifulco, Rheol. Acta **36**, 406 (1997).
[19] K. H. de Haas, D. van den Ende, C. Blom, E. G. Altena, G. J. Beukema, and J. Mellema, Rev. Sci. Instrum. **69**, 1391 (1998).
[20] S. Comas-Cardona and C. L. Tucker III, J. Rheol. **45**, 259 (2001).
[21] B. J. Berne and R. Pecora, *Dynamic Light Scattering* (Wiley, New York, 1976).
[22] A. Knaebel, M. Bellour, J. P. Munch, V. Viasnoff, F. Lequeux, and J. L. Harden, Europhys. Lett. **52**, 73 (2000).
[23] V. Viasnoff, F. Lequeux, and D. J. Pine, Rev. Sci. Instrum. **73**, 2336 (2002).
[24] R. H. Tromp, F. van de Velde, J. van Riel, and M. Paques, Food Res. Int. **34**, 931 (2001).
[25] E. ten Grotenhuis, M. Paques, and G. A. van Aken, J. Colloid Interface Sci. **227**, 495 (2001).
[26] Y. Nicolas, A. Knaebel A, R. Skouri, T. B. J. Blijdenstein, M. Paques, and J.-P. Munch (unpublished).
[27] F. Scheffold, S. E. Skipetrov, S. Romer, and P. Schurtenberger, Phys. Rev. E **63**, 61404 (2001).
[28] T. B. J. Blijdenstein, Y. Nicolas, E. van der Linden, T. van Vliet, M. Paques, G. A. van Aken, A. Knaebel, and J.-P. Munch, Proceedings of Zurich 2003.
[29] S. Guido and M. Villone, J. Rheol. **42**, 395 (1998).
[30] A. Egner, V. Andresen, and S. W. Hell, J. Microsc. **206**, 24 (2002).